Cryobiology 111 (2023) 9–15

Contents lists available at ScienceDirect

Cryobiology

journal homepage: www.elsevier.com/locate/cryo

Is isochoric vitrification feasible?

Prem K. Solanki, Yoed Rabin *

Biothermal Technology Laboratory, Department of Mechanical Engineering, Carnegie Mellon University, Pittsburgh, PA, 15213, USA

ARTICLE INFO

Keywords:
Isochoric cryopreservation
Vitrification
Mathematical modeling
Computation

ABSTRACT

This study investigates the feasibility of ice-free isochoric vitrification for cryopreservation applications using mathematical modeling, computation tools, and the underlying principles of thermo-mechanics. This study is triggered by an increasing interest in the possibility of isochoric vitrification, following promising experimental results of isochoric cryopreservation. In general, isochoric cryopreservation is the preservation of biological materials in subzero temperatures in a rigid-sealed container, where some ice crystallization creates favorable pressure elevation due to the anomaly of water expansion upon ice Ih formation. Vitrification on the other hand is the transformation of liquid into an amorphous solid in the absence of any crystals, which is typically achieved by rapid cooling of a highly viscous solution. The current study presents a mathematical model for vitrification under variable pressure conditions, building upon a recently published thermo-mechanics modeling approach for isochoric cryopreservation. Using the physical properties of dimethyl sulfoxide (DMSO) as a representative cryoprotective agent (CPA), this study suggests that vitrification under isochoric conditions is not feasible, essentially since the CPA solution contracts more than the isochoric chamber by an order of magnitude. This differential contraction can lead to absolute zero pressure in the isochoric chamber, counteracting the premise of the isochoric cryopreservation process. It is concluded that the only alternative to prevent ice formation while benefiting from the potential advantages of higher pressures is to create the required pressures by external means, and not merely by passively enclosing the specimen in an isochoric chamber.

1. Introduction

Vitrification is the most promising alternative for indefinite storage of large-size biological tissues and organs in cryogenic temperature, where *vitrification* means transformation into a *glassy* or amorphous solid [12]. It is emphasized that the term vitrification is used throughout this study to signify an ice-free state, whereas the literature term of *partial vitrification* often means the coexistence of vitrified and crystallized material. Isochoric (i.e., constant-volume) cryopreservation, or the preservation of biological materials in a rigidly sealed container has been explored in recent years, where natural pressure elevation helps in limiting the extent of crystallization [29,36,47]. An experimental study aimed at providing a proof-of-concept that the underlying concepts of vitrification and isochoric preservation can be integrated was presented recently [49].

Vitrification is achieved by loading the tissue with cryoprotective agents (CPAs), which exhibit exponential increase in viscosity with the decreasing temperature [25]. The viscosity of that CPA varies from water-like value at room temperature, and up to such a high value in cryogenic temperatures, that it behaves as a solid within any practical timescale. The threshold below which the CPA behaves like a solid is known as the glass transition temperature (T_g). If the CPA is cooled fast enough, such that the timescale to form ice is longer than the time window to reach the glass transition temperature, crystallization can be avoided, and the material can reach a pure vitreous state. Due to temperature gradients, the tendency of the material to change volume with the decreasing temperature, and the underlying principles of solid mechanics, thermo-mechanical stresses may develop in the material during vitrification [42–44]. When these stresses exceed the strength of the material, structural damage follows, with fracture formation as the most notable outcome [33,34]. The tendency to change volume with temperature is represented by the thermo-physical property of thermal expansion coefficient [39].

Most commonly, cryopreservation processes are conducted under standard atmospheric surrounding conditions, while the added benefits of elevated pressure to avoid ice crystallization have been demonstrated [11,12,45,46]. In general, increasing the pressure lowers the homogeneous nucleation temperature and elevates the glass transition

* Corresponding author.
E-mail address: rabin@cmu.edu (Y. Rabin).

https://doi.org/10.1016/j.cryobiol.2023.03.007
Received 31 January 2023; Received in revised form 16 March 2023; Accepted 18 March 2023
Available online 21 March 2023

temperature, which in turn reduces the CPA concentration and cooling rate required to achieve vitrification [21]. A lower concentration of the CPA also lowers the critical rewarming rate required to avoid rewarming-phase crystallization (RPC) [14], potentially leading to lower thermo-mechanical stresses [40].

Isochoric cryopreservation refers to a special class of high-pressure cryopreservation [36], where the pressure elevates due to the anomaly of water expansion upon ice Ih formation [4], while the specimen is contained in a stiff sealed container. Due to the Le Chatelier's principle [31], the increased pressure with the decreasing temperature limits further ice crystallization, thereby creating a self-limiting ice formation process. At equilibrium, the relation between temperature and pressure in a pure water system is given by the liquidus curve on the phase diagram, denoted by the red line in Fig. 1 [16]. The harmful effects of ice crystallization on the cryopreserved specimen could be avoided if the specimen is located within the unfrozen portion of the isochoric vessel at all times [36,47].

The application of isochoric freezing is not limited to pure water systems, whereas CPAs dissolved in water can further assist by modulating ice formation. The presence of CPAs is expected to lower the overall pressure in the isochoric system at any given temperature, due to the lower crystallization rate of the mixture. Furthermore, ice crystallization would increase the concentration of the remaining CPA solution, further suppressing the tendency of the remaining solution to crystallize. Isochoric cryopreservation has been demonstrated as an effective process for short-to medium-term preservation of tissues, organs, and food products, within a temperature range bounded by the melting temperature of pure water and the liquidus curve of the CPA solution [1,2,23,28,30,48].

A proof-of-concept study was published recently [49], aiming at achieving vitrification under isochoric conditions. There, the authors hypothesized that the pressure should remain unchanged during the isochoric vitrification process, while the effect of thermal expansion of the container on the pressure within the system can be neglected. Furthermore, pressure increase during rewarming was presented there as a measure of the degree of devitrification when it does take place. Based on the above hypothesis [49] and in comparison with vitrification in standard atmospheric conditions (i.e., in an open container), it was concluded that isochoric vitrification requires: (i) substantially lower CPA concentration, and (ii) less expensive chambers, having thinner walls to support the lower pressures. That publication [49] creates an excellent platform for sharing research analysis approaches and techniques, while debating the associated physical phenomena. In this context and in the absence of visual or other direct observations, the authors of the current study recruited mathematical modeling and computation tools to investigate the feasibility of isochoric vitrification concept. Specifically, the current study is based on a thermo-mechanics model, which was recently developed for general isochoric processes [41].

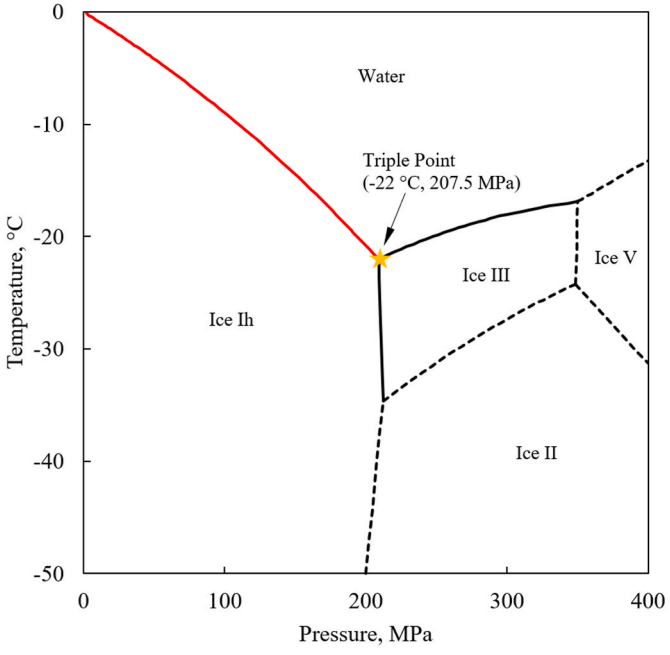

Fig. 1. Temperature-pressure phase diagram of pure water [16].

2. Problem definition and mathematical formulation

A simplified spherical container with an infinitely rigid wall is assumed in this study, Fig. 2. This geometry is a practical choice, following the notion that the ability to achieve a vitrification state is shape independent, while avoiding the unnecessary discussion about container geometries and preferences. The modeling approach taken here has recently been developed for isochoric cryopreservation where some crystallization does occur [41]. That model treats the contained material as having a viscoelastic behavior (i.e., the constitutive law), which is the expected material behavior from a vitrifying material [10,33,40,42]. Furthermore, it is explained there how to include crystallization during isochoric cooling [41]. Below are the key modeling elements in brief, for the completion of presentation.

2.1. Heat transfer model

The heat transfer model assumes conduction throughout the domain, while heat generation due to viscous dissipation is neglected [17]:

$$\rho C_p \dot{T} = \nabla\cdot(k\nabla T) \tag{1}$$

where ρ is the density, C_p is the specific heat at constant pressure, T is the temperature, and k is the thermal conductivity. The Einstein model for internal energy storage is used to approximate the temperature-dependent specific heat [13]:

$$C_p \cong C_v = \frac{3N\kappa_b}{M_u}\left(\frac{\theta_E}{T_a}\right)^2 exp\left(\frac{\theta_E}{T_a}\right)\left[exp\left(\frac{\theta_E}{T_a}-1\right)\right]^{-2};\ \theta_E = \frac{\hbar\omega_m}{\kappa_b} \tag{2}$$

where C_v is the specific heat at constant volume, N is the number of oscillators, κ_b is the Boltzmann constant (1.38×10^{-23} J/K), M_u is the molecular weight, T_a is the absolute temperature, θ_E is the Einstein temperature, $\hbar$ is the reduced Planck's constant (1.054×10^{-34} J s), and ω_m is the frequency of oscillation of the molecule (6.415×10^{13} Hz)

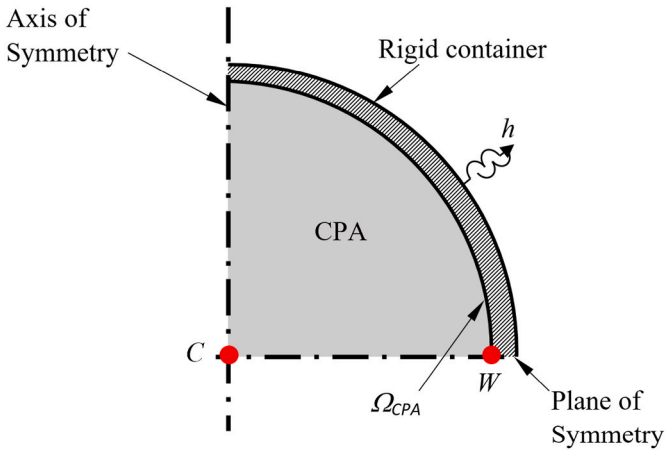

Fig. 2. Schematic illustration of the simplified spherical isochoric chamber used in the current study, where points C and W refer to the center and the surface of the CPA domain, respectively.

[13]. The Einstein model has been demonstrated as a good approximation for the specific heat of amorphous materials (such as glasses) [7]. Moreover, since the lack of long-range order among the molecules of liquids resembles that in amorphous materials, the Einstein model was used to approximate the specific heat for 7.05 M DMSO from room temperature, where the CPA behaves as a liquid, down to temperatures below Tg [13]. Although the Einstein model describes the specific heat at constant volume (C_v), its deviation from the specific heat at constant pressure (C_p) is less than 1% within the temperature range of available relevant literature data [13,38].

The heat transfer between the outer surface of the specimen and the cooling environment is described using convective heat transfer [18]:

$$-k\frac{dT}{d\hat{n}} = h(T_W - T_\infty) \tag{3}$$

where $\hat{n}$ is a unit normal to the wall, and h is the heat transfer coefficient between the outer surface of the isochoric chamber and the cooling environment, denoted by subscripts W and ∞, respectively. The heat transfer coefficient is considered to be 350 W/m^{2}K, selected to recreate conditions inside a Planar Kryo-10 controlled-rate cooler as a cooling environment [13] as an example. Nonetheless, the conceptual outcome of this study is independent of this value.

2.2. Solid mechanics formulation

The vitrified material is modeled as a Maxwell fluid, where the total strain rate is [9,40,42]:

$$\dot{\boldsymbol{\varepsilon}}_{total} = \dot{\boldsymbol{\varepsilon}}_{creep} + \dot{\boldsymbol{\varepsilon}}_{elastic} + \dot{\boldsymbol{\varepsilon}}_{thermal} \tag{4}$$

where the creep, elastic, and thermal strain rates are calculated by:

$$\dot{\boldsymbol{\varepsilon}}_{creep} = \frac{\boldsymbol{S}}{2\eta} \tag{5}$$

$$\dot{\boldsymbol{\varepsilon}}_{elastic} = \frac{1}{E}[(1+\nu)\dot{\sigma} - \nu \boldsymbol{I}\cdot\boldsymbol{tr}(\dot{\sigma})] \tag{6}$$

$$\dot{\boldsymbol{\varepsilon}}_{thermal} = \frac{\mathrm{d}\boldsymbol{\varepsilon}_{thermal}}{\mathrm{dt}} \tag{7}$$

where $\boldsymbol{S}$ is the deviatoric stress tensor, η is the viscosity, E is the elastic modulus, ν is the Poisson ratio, $\boldsymbol{I}$ is the identity matrix, and $\boldsymbol{tr}$ is the trace of a matrix.

To enforce isochoric conditions on the specimen, the outer surface of the container is constrained to zero displacement:

$$\boldsymbol{u}(\Omega_{CPA}) = 0 \tag{8}$$

where $\boldsymbol{u}$ is the displacement tensor and Ω_{CPA} is the outer boundary of the CPA domain (Fig. 2).

The pressure is defined as the average normal stress in the solution of the mechanics problem:

$$P = -\frac{1}{3}\sum_1^3 \sigma_{ii} \tag{9}$$

where the three normal stress components in a stationary fluid are identical and equal to the hydrostatic pressure.

2.2.1. Material properties

Dimethyl Sulfoxide (DMSO) is selected as a reference vitrification solution in this study at a concentration of 7.05 M [27,35]. DMSO is a key ingredient in many CPA solutions for cryopreservation by vitrification [27]. In practice, 7.05 M DMSO displays viscoelastic behavior with exponentially increasing viscosity as the cooling progresses [25] (Table 1). Pressure dependency of the thermophysical properties is not considered in this study, due to lack of sufficient data. Notably, by far the most significant pressure-dependent effect during isochoric partial crystallization is the melting of pure water ice [36,41], which is to be avoided in an ideal vitrification process.

Table 1
Material properties of 7.05 M DMSO used in the current study as a representative CPA used for vitrification.

Property	Value		
Viscosity, Pa·s	1.77×10^4	$-106\ ^\circ\mathrm{C} \le T$	[25]
	$2.8190 \times 10^{-27}\ e^{-0.6447\ T}$	$-143\ ^\circ\mathrm{C} \le T < -106\ ^\circ\mathrm{C}$	
	4.06×10^{14}	$T \le -143\ ^\circ\mathrm{C}$	
Glass transition temperature, °C	−132		[24]
Density, kg/m^3	1100		[20]
Thermal conductivity, W/m °C	$-2.95 \times 10^{-10}T^4 - 6.87 \times 10^{-8}T^3 - 1.29 \times 10^{-6}T^2 + 7.42 \times 10^{-4}T + 0.356$		[8]
Specific heat, J/kg °C	Eq. (4)		[13]
Thermal Strain	$5.63 \times 10^{-8}T^2 + 2.08 \times 10^{-4}T - 4.46 \times 10^{-3}$		[32]
Young's modulus, MPa	$2.38 \times 10^{-7}\ e^{-1.663\ T} + 49.9$	$-132\ ^\circ\mathrm{C} \le T < 25\ ^\circ\mathrm{C}$	[19]
	800	$T \le -132\ ^\circ\mathrm{C}$	
Poisson's ratio	0.25		[9]

The thermal strain $\boldsymbol{\varepsilon}_{thermal}$ for pure 7.05 M DMSO was measured previously using a proprietary measurement device between room temperature and −95.8 °C, with the functional behavior listed in Table 1. Based on experimental data, 7.05 M DMSO is demonstrated to undergo contraction in this temperature range, which translates to a monotonically decreasing thermal strain [32]. The thermal strain below this temperature is extrapolated using quadratic extrapolation. Note that thermal strain of tissues permeated with 7.05 M DMSO is available in the literature [20,32].

While 7.05 M DMSO is used as a reference solution in the current study, the main conclusions of this study are independent of the CPA concentration, as discussed below.

2.3. Thermal protocol

A representative vitrification thermal protocol for 7.05 M DMSO is selected for this study, as displayed in Fig. 3: (C_1) fast cooling at a rate of 5 °C/min between an initial temperature of 20 °C and −122 °C; (H_1) annealing temperature hold at −122 °C, which is 10 °C above the glass transition temperature (T_g = −132 °C, Table 1); (C_2) slow cooling at a rate of 1 °C/min to the storage temperature of −196 °C; (H_2) storage

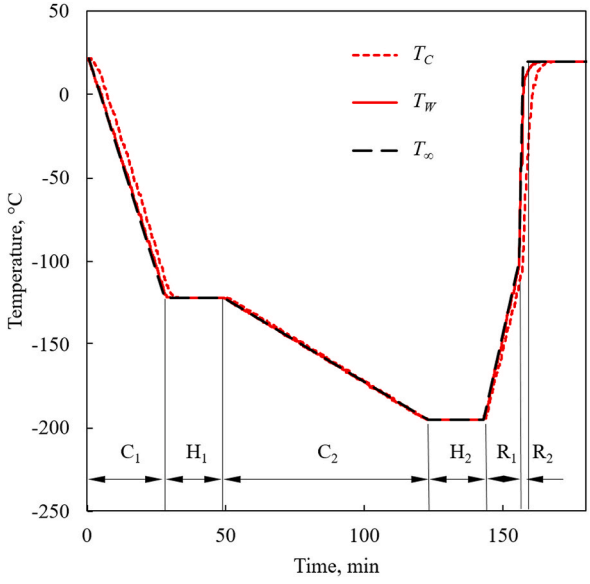

Fig. 3. Thermal histories at the center, T_C, and surface the boundary of the CPA domain, T_W, while the cooling environment is represented by T_∞.

temperature hold at −196 °C; (R_1) slow rewarming at a rate of 7.5 °C/min up to −100 °C; and (R_2) fast rewarming at a rate of 100 °C/min back to room temperature. Segments H_1 and H_2 are sufficiently long to approach thermal and pressure equilibrium across the domain. While virtually an infinite number of thermal protocol parameters could be selected to specify the above thermal protocol for the purpose of the current study, the specific choice of values does not affect the generality of the conclusions drawn below.

2.4. Computer modeling

The thermo-mechanics coupled problem is solved incrementally, by sequentially solving the heat transfer and solid mechanics problems, using the commercial FEA code COMSOL Multiphysics [6]. For this purpose and due to the spherical symmetry of the problem, only one quadrant of the sphere is simulated, using 7000 biquadratic elements with the commercial finite element analysis (FEA) code COMSOL Miltiphysics ® [5].

3. Results and discussions

3.1. Mathematical modeling

The temperature and pressure histories in a spherical container having a diameter of 10 mm, in which the CPA undergoes complete vitrification, are displayed in Figs. 3 and 4, respectively. The surface of the specimen, T_W, closely follows the temperature of the cooling surrounding environment, T_∞, while the center of the specimen lags behind due to the low thermal conductivity of 7.05 M DMSO [8]. During cooling and rewarming, the maximum temperature difference between the surface and center of the specimen is 12.5 °C and 94.2 °C, respectively. The maximum temperature difference in the specimen is observed at the onset of fast rewarming (R_2) when the surface of the specimen experiences sudden rapid rewarming while the center of the specimen is much slower to respond.

It can be observed from Fig. 4 that the pressure only decreases with temperature during cooling when ice crystallization is assumed to not take place. This can be easily explained by the fact that the thermal expansion coefficient of the CPA is larger than that of the container wall, while the isochoric chamber wall is assumed to be infinitely rigid.

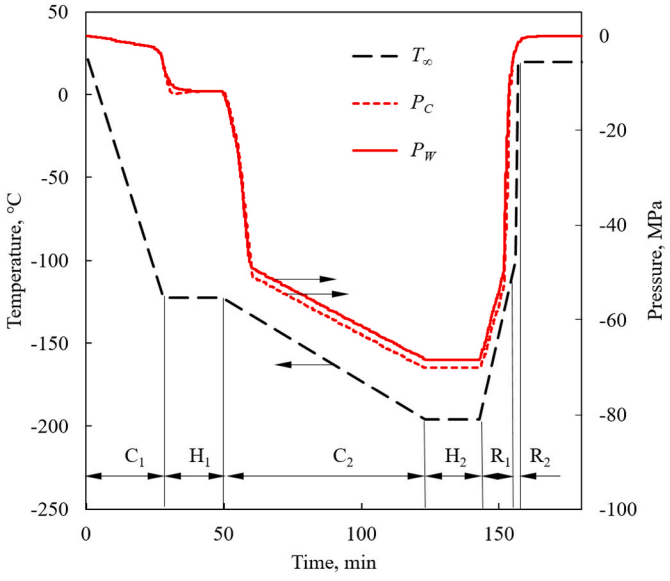

Fig. 4. Pressure history at the center, P_C, and the surface, P_W, of the CPA domain undergoing vitrification, where negative pressure signifies tension in solids.

Higher thermal expansion coefficient means larger strains with the change of temperature, where the thermal expansion coefficient is a physical property having a positive value only. It is the direction of change in temperature which dictates whether the accumulated effect would result in contraction or expansion. When expansion or contraction are constrained, pressure will increase or decrease to make deformation compatible across the domain.

A pressure variation between the wall and the center of the container can be first observed at the beginning of the stress relaxation segment (i.e., the onset of segment H_1), Fig. 4, which corresponds to the temperature gradient across the CPA at that time. Note that although the temperatures are above T_g throughout the domain during segment H_1, the stress distribution, and consequently the pressure distribution may already develop at that time [33]. The temperature below which the material may develop significant stresses has been defined as the set-temperature, T_s [33], which is strain-rate dependent – it increases with the increasing strain rate (i.e., the rate of loading). A temperature range of the order of 10 °C may be expected between the T_s and T_g under some conditions related to cryopreservation by vitrification [33]. In fact, the purpose of segment H_1 is to allow for the strain to relax across the domain before surpassing T_g. The maximum pressure variation at the onset of segment H_1 is 1.76 MPa, which dissipates to a pressure variation of 0.176 MPa (10% of its initial value) in 8.4 min. The pressure variation eventually reduces to negligible values as segment H_1 continues.

While previous computational studies of vitrification under isobaric conditions have considered a temperature-independent elastic modulus for the CPA [9,40,42], this assumption may become weak under isochoric conditions due to the stress history development. The reason for this assumption in prior studies is that the specimen does not experience significant stresses in high cryogenic temperatures, when the viscosity value is low and when the material behaves like a free-to-flow fluid. By contrast, higher stresses develop in isochoric preservation in higher temperature, and the temperature-dependency of the elastic modulus cannot be neglected anymore (Table 1).

Now that the distinction between stress development in a fluid-like material and a solid-like material has been made, it is crucial to take a step back and evaluate the magnitude of the pressures displayed in Fig. 4. It is clear that the pressure predictions in Fig. 4 are grossly nonphysical, where the pressure is presented relatively to the reference pressure when the chamber was sealed (i.e., gauge pressure) and hence the negative sign signifies below atmospheric pressure. If the isochoric container is sealed at a standard atmospheric pressure (i.e., 0.101 MPa), its pressure cannot go below −0.101 MPa pressure gauge (i.e., complete vacuum), whereas Fig. 4 suggests negative pressures of the order of 70 MPa. Furthermore, the pressure decrease to a complete vacuum occurs 115 s from the onset of cooling, corresponding to an outer surface temperature drop of 8 °C from its initial condition. While a negative absolute pressure is clearly nonphysical, it begs the question of what might possibly take place within the isochoric chamber as the pressure decreases and approaches vacuum conditions.

There may be many possible scenarios for the events occurring when the CPA approaches vacuum conditions, however two physical phenomena may dominate the process, both leading to the formation of microbubbles: cavitation [3,37] and degasification [15,22]. Cavitation is a phenomenon in which the static pressure of a liquid reduces to below the liquid's vapor pressure, leading to the formation of small vapor-filled cavities in the liquid (the same material in the vapor bubbles and the surrounding liquid), whereas degasification is the removal of dissolved gases, such as oxygen, from liquids (gas bubbles of a different material than the surrounding liquid). Either way, such bubbles can serve as nucleators for the formation of water ice [26], which can negate the attempt to achieve the ice-free state of vitrification.

Although negative absolute pressure in free-to-flow fluids is nonphysical, negative normal stresses in solids violates no physical law (recall that normal stress in a stationary fluid is defined as pressure, Eq. (9)). Negative normal stress in solids is defined as tensile stress, and its

upper limit is defined by the strength of the material, which is a physical property varying among different materials. It is well established that the vitrified material can be modeled as a linear-elastic solid below glass transition [25,33,44], and hence the pressure values in Fig. 4 provide insight into the thermo-mechanics process in those lower temperatures. For example, the pressure variation observed in the CPA at lower temperatures can be attributed to differential thermal contraction in the CPA as different layers of the linear-elastic solid contract at different rates in response to the temperature gradients [44]. The maximum pressure variation within the specimen during cooling and rewarming is 3.1 MPa and 12.5 MPa, respectively.

Since the stress during monotonic cooling of a solid is cumulative, one can estimate the tensile stress magnitude at storage as the increase of stress between the glass transition and the storage temperatures. It can be seen from Fig. 4 that the corresponding difference is of the order of 55 MPa. Unfortunately, the tensile strength of vitrified CPAs is of the order of a few MPa only [33], which would result in structural damage to the CPA. In practice, this may result in a series of fractures within the domain, each generated when the local stress reaches the yield strength of the material. It is quite difficult to project where the first fracture would occur and how it would progress, but the potential of destructive outcome across the domain is major.

3.2. Comparison with experimental literature data

A recent study aimed at providing a proof-of-concept for isochoric vitrification, using propanediol (PD) and DMSO water-based solutions as CPAs [49]. That study included either a multi-step cooling protocol, or direct immersion of the isochoric chamber in a liquid nitrogen (LN_2) bath to achieve the rapid cooling required to facilitate vitrification. That study generally demonstrated that under repeated identical conditions, the elevated pressure magnitude decreases with the increasing CPA concentration to the point that only marginal pressure is being detected. For example, in a series of isochoric chamber immersion in LN_2, the pressure decreased from a maximum level of 200 MPa with 10% PD solution to the order of a few MPa with 30% PD during cooling. Both cases showed evidence of crystallization during rewarming. In a different set of stepwise controlled cooling in 40 °C decrements, the pressure magnitude dropped from a level of 220 MPa–47 MPa for 10% and 30% PD solution, respectively. The trends remain the same when switching from PD to DMSO solutions, although the pressure levels varied.

As the concentration of CPAs is further increased to 44% PD in one experiment and to 35% DMSO in another experiment, the maximum pressure is reported to decrease below 5 MPa [49]. For 49% DMSO, the authors there reported on a further maximum pressure decrease to below 3 MPa, while the reference solution of 7.05 M DMSO in the current study represents a concentration of 50.2%. Based on comparison with the pressure increase at lower concentrations of PD and DMSO, and the sensitivity of the pressure transducer below 5 MPa, the authors of [49] have concluded that a complete ice-free state was achieved when the isochoric chamber containing 44% PD or 35% DMSO was cooled to cryogenic temperatures. According to the previous study [49], these concentrations of CPA were sufficient to achieve isochoric vitrification using both cooling protocols – controlled cooling in 40 °C decrements, and rapid cooling by plunging in LN_2,.

Critical to the current discussion, the authors of the experimental study [49] reported on pressure increase in all experiments, while the results of the current mathematical analysis suggest that vitrification must result in pressure decrease. The question is how to reconcile results of the previous and the current studies, assuming that the constitutive model and the physical properties used in the current study are representative. In higher temperatures, it is quite possible that limited ice crystallization does take place, nucleated by microbubbles, just in the right amount to maintain the observed single digit MPa pressure. Furthermore, since ice Ih expands upon freezing in temperatures above the triple point of water displayed in Fig. 1 (liquid, ice Ih and ice III at −22 °C [4]), ice crystals can possibly counteract the formation of bubbles to maintain constant pressure. In essence, this maybe a self-limiting effect of ice formation, where this term takes a different meaning than that in the context of isochoric preservation [31]. Of course, this is only one plausible explanation, which does not preclude other possibilities.

At lower temperatures, when the CPA behaves like a solid, the reason for the discrepancy between the results of the previous study [49] and the outcome of the current modeling study must be different. This may be a compounded reason associated with the mechanical behavior of glasses and the specific experimental setup. While the experimental study reports on pressures measured down to −180 °C, the pressure transducer used there is designed for free-to-flow fluids only, and the vitrified material behaves as a solid below T_g in any practical time scale [25]. Considering the fluidity of the CPA, pressure measurements with that transducer (HP1000 series, SUCO ESI, Boca Raton, FL, USA) can only be done above $T_g = -115$ °C and $T_g = -133$ °C for PD and DMSO, respectively. In fact, the CPA will stop flowing freely above T_s as already discussed above. Furthermore, if the pressure transducer is immersed in the cooling environment (the controlled-rate cooling chamber of the experimental setup for example), it cannot reliably measure pressures below −40 °C according to its specifications.

The above discussion does not imply that vitrification is not possible under high pressure conditions. By application of high pressure using mechanical devices, a previous study has demonstrated that the concentration of the glass forming material required to achieve vitrification can be reduced [21]. In this context, the increased pressure by the mechanical device in Ref. [21] would offset the tendency of the glass forming material to contract, and thereby create favorable conditions for vitrification. The mathematical framework presented in the current study is suitable for the analysis of such externally pressurized systems as well.

3.3. Void volume due to thermal contraction during vitrification

Calculating the amount of ice that must form before the pressure elevates in a partial vitrification process in an isochoric chamber is quite complex, given the nature of bubbles formation, the kinetics of crystallization in low pressures, and transient thermo-mechanics effects. However, it is possible to first-order approximate the maximum void volume that would have been created due to thermal contraction, if indeed complete vitrification has taken place in an isochoric chamber. This approximation is based on the following simplified assumptions: (i) the thermal expansion of CPA in lower pressures remains the same as in standard atmospheric pressure; (ii) the thermal expansion of the isochoric chamber (steel) is an order of magnitude smaller than that of the CPA; (iii) the CPA is free to flow as a Newtonian fluid within the temperature range of interest; (iv) the fluid domain is cooled uniformly; and (v) the isochoric chamber is sealed at 20 °C, while absolute zero pressure is reached at 12 °C, as discussed in one of the examples above.

It was found experimentally that 7.05 M DMSO can flow freely under similar vitrification conditions down to at least −95.8 °C [32]. The linear thermal strain of 7.05 M DMSO between 12 °C and −95.8 °C is 2.19%, resulting in a volumetric strain of 6.43%, which would be the overall bubbles volume (i.e., the maximum void volume) based on the above assumptions. If 7.05 M DMSO is further assumed to be cooled as a free-to-flow fluid down to the so-called *set temperature* of −122 °C (10 °C above $T_g = -132$ °C) [33], the linear thermal strain would be 2.73% (based on a quadratic extrapolation below −95.8 °C) and the maximum void volume would increase to 7.97%. Based on a follow-up study on blood vessels permeated with 7.05 M DMSO [20], the corresponding volumetric strain would be 3.99% and 5.30% for the same end temperatures of −95.8 °C and −122 °C (this time with no extrapolation), respectively. Obviously, in a real process, the biological sample would be surrounded by a large amount of pure solution, and the actual void volume would be a weighted average of the above values.

Notably for the case of pure 7.05 M DMSO cooled to −95.8 °C as an example, it is not only that the total amount of crystals would have to reach 6.43% before pressure elevation is sensed, but that the difference between volume contraction of the remaining liquid and the volume expansion of the forming crystals must exceed that 6.43% value – this would translate to a massive amount of crystals. To put this number into perspective, recall that pure water expands by 9% upon freezing in standard conditions (or compressed by 9% if expansion is prohibited), and that about 50% of the 7.05 M DMSO is pure water before cooling.

Unfortunately, the above first-order analysis falls short of predicting the precise volume of crystals that is required to drive pressure elevation. A more detailed analysis must be employed for this purpose, accounting for the kinetics of crystallization in an ever-changing CPA concentration (due to the formation of ice), under low pressures, and subject to a nonuniform and transient temperature field. Nonetheless, it is clear from the above first-order analysis that the inability to sense pressure elevation in and of itself cannot serve as an indication for the absence of a crystalized material, the amount of which can be quite significant.

4. Summary and conclusions

Isochoric cryopreservation is a promising approach for the preservation of biological materials in low temperatures, which benefits from decreased ice formation with the increasing pressure in a sealed-rigid container. Recent experimental studies have demonstrated the potential benefits of isochoric cryopreservation for tissue and organ banking, as well as for the preservation of food products. Not surprisingly, with exclusive experimental measurements of macro-level indicators on the one hand, and with the inability to make direct experimental observations at the micro-level on the other hand, opinions and speculations are often recruited to assist in rationalizing the cryopreservation outcome. In this context, *macro-level* means the entire isochoric system, which is thus far exclusively characterized by a lumped temperature and a lumped pressure measured somewhere in the container, while *micro-level* refers to the distributed phenomena of ice formation, temperature field, and the nine-components stress tensor field. To the best of our knowledge, no isochoric cryopreservation system has been presented thus far which facilitates micro-level isochoric observations. In effort to assist in bridging this gap of knowledge, the current study utilizes mathematical modeling, computation tools, and the underlying principles of thermo-mechanics.

The current study presents a mathematical model for vitrification under variable pressure conditions, building upon a recently published thermo-mechanics modeling approach for isochoric cryopreservation [41]. The current study suggests that complete vitrification under isochoric conditions is not likely to take place, essentially since the CPA solution contracts more than the isochoric chamber in the absence of water crystallization. This would lead to a decreasing rather than an increasing of pressure with the decreasing temperature inside the chamber, resulting in two adverse effects: (i) counteracting the protective effect attributed to pressure elevation on the cryopreserved biomaterial, and (ii) promoting rather than suppressing ice nucleation, which in turn would require even faster cooling rates to facilitate vitrification.

When crystallization is assumed to be prevented in the isochoric chamber, the pressure must rapidly decrease early on in the isochoric process, probably yielding the formation of microbubbles as the absolute pressure approaches zero (i.e., vacuum). It is difficult to imagine that those microbubbles would not serve as extremely favorable nuclei for ice formation. Furthermore, when microbubbles fuse to fewer but larger bubbles, an increased ice growth rate can be expected on their expanding surfaces. Based on a first-order analysis, it is demonstrated in this study that a significant amount of ice may form in the isochoric chamber before its pressure would elevate. If follows that the pressure alone cannot be used as a measure of the quality of vitrification.

It seems that the only alternative to facilitate the ice-free state of vitrification while benefiting from the presumed advantages of higher pressures is to create the required pressures by external means. By no means does this study come to argue that results of prior experimental studies designated by their authors as isochoric vitrification are invalid in terms of tissue viability, functionality, and other possible cryobiology measures. However, this study questions the designation of those reported experiments as isochoric vitrification. Notably, the current study is not about semantics but about attributing the correct physical phenomena to experimental measurements, in effort to develop better cryopreservation solutions, devices and processes.

Acknowledgements

Research reported in this paper was supported in parts by the National Institute of Allergy and Infectious Diseases (NIAID) of the National Institutes of Health under (NIH) award number 9R44 AI145782, and by the National Science Foundation (NSF) award number EEC 1941543. This research was also supported in part by Sylvatica Biotech Inc. The content of this paper is solely the responsibility of the authors and does not necessarily represent the official views of the NIH, NSF, or Sylvatica Biotech Inc.

References

[1] C. Bilbao-Sainz, A.G.J. Sinrod, L. Dao, G. Takeoka, T. Williams, D. Wood, D. F. Bridges, M.J. Powell-Palm, G. Ukpai, B.-S. Chiou, V.C.H. Wu, B. Rubinsky, T. McHugh, Preservation of spinach by isochoric (constant volume) freezing, Int. J. Food Sci. Technol. 55 (2020) 2141–2151, https://doi.org/10.1111/IJFS.14463.
[2] C. Bilbao-Sainz, A. Sinrod, M.J. Powell-Palm, L. Dao, G. Takeoka, T. Williams, D. Wood, G. Ukpai, J. Aruda, D.F. Bridges, V.C.H. Wu, B. Rubinsky, T. McHugh, Preservation of sweet cherry by isochoric (constant volume) freezing, Innovat. Food Sci. Emerg. Technol. 52 (2019) 108–115, https://doi.org/10.1016/J.IFSET.2018.10.016.
[3] F. Caupin, E. Herbert, Cavitation in water: a review, Compt. Rendus Phys. 7 (2006) 1000–1017, https://doi.org/10.1016/J.CRHY.2006.10.015.
[4] V.E. Chizov, O.V. Nagornov, Thermodynamic properties of ice, water and their mixture under high pressure, in: Glaciers-Ocean-Atmosph. Interact, Proceedings Int. Symp)., St. Petersburg, 1990, pp. 463–470.
[5] COMSOL AB, Meshing, in: COMSOL Multiphysics Ref. Man., COMSOL Multiphysics® V. 5.6, 2020, pp. 662–749. Stockholm, Sweden.
[6] COMSOL AB, COMSOL Multiphysics® v5.6 (n.d.), www.comsol.com.
[7] D.G. Cahill, R.O. Pohl, Lattice vibrations and heat transport in crystals and glasses, Annu. Rev. Phys. Chem. 39 (2003) 93–121, https://doi.org/10.1146/ANNUREV.PC.39.100188.000521.
[8] L.E. Ehrlich, J.S.G. Feig, S.N. Schiffres, J.A. Malen, Y. Rabin, Large thermal conductivity differences between the crystalline and vitrified states of DMSO with applications to cryopreservation, PLoS One 10 (2015), e0125862, https://doi.org/10.1371/journal.pone.0125862.
[9] D.P. Eisenberg, P.S. Steif, Y. Rabin, On the effects of thermal history on the development and relaxation of thermo-mechanical stress in cryopreservation, Cryogenics 64 (2014) 86–94, https://doi.org/10.1016/j.cryogenics.2014.09.005.
[10] D.P. Eisenberg, M.J. Taylor, J.L. Jimenez-Rios, Y. Rabin, Thermal expansion of vitrified blood vessels permeated with DP6 and synthetic ice modulators, Cryobiology 68 (2014) 318–326, https://doi.org/10.1016/j.cryobiol.2014.04.010.
[11] G.M. Fahy, D.I. Levy, S.E. Ali, Some emerging principles underlying the physical properties, biological actions, and utility of vitrification solutions, Cryobiology 24 (1987) 196–213, https://doi.org/10.1016/0011-2240(87)90023-X.
[12] G.M. Fahy, D.R. MacFarlane, C.A. Angell, H.T. Meryman, Vitrification as an approach to cryopreservation, Cryobiology 21 (1984) 407–426, https://doi.org/10.1016/0011-2240(84)90079-8.
[13] J.S.G. Feig, P.K. Solanki, D.P. Eisenberg, Y. Rabin, Polarized light scanning cryomacroscopy, part II: thermal modeling and analysis of experimental observations, Cryobiology 73 (2016) 272–281, https://doi.org/10.1016/j.cryobiol.2016.06.004.
[14] Z. Han, J.C. Bischof, Perspective: critical cooling and warming rates as a function of CPA concentration, Cryo-Letters 41 (2020) 185–193.
[15] W. Henry, Experiments on the quantity of gases absorbed by water, at different temperatures, and under different pressures, Philos. Trans. R. Soc. London, A 93 (1803) 29–274, https://doi.org/10.1098/RSTL.1803.0004.
[16] P.V. Hobbs, Ice Physics, Oxford University Press, 2010.
[17] J.P. Holman, Unsteady-state conduction, in: Heat Transf, Mc-Graw Hill, New York, NY, 2010, pp. 139–214.
[18] J.P. Holman, Heat Transfer, McGraw Hill Higher Education, 2010.
[19] J.L. Jimenez Rios, P.S. Steif, Y. Rabin, Stress-strain measurements and viscoelastic response of blood vessels cryopreserved by vitrification, Ann. Biomed. Eng. 35 (2007) 2077–2086, https://doi.org/10.1007/s10439-007-9372-0.

[20] J.L. Jimenez Rios, Y. Rabin, Thermal expansion of blood vessels in low cryogenic temperatures, part II: vitrification with VS55, DP6, and 7.05M DMSO, Cryobiology 52 (2006) 284–294, https://doi.org/10.1016/j.cryobiol.2005.12.006.
[21] H. Kanno, C.A. Angell, Homogeneous nucleation and glass formation in aqueous alkali halide solutions at high pressures, J. Phys. Chem. 81 (1977) 2639–2643, https://doi.org/10.1021/J100541A013/ASSET/J100541A013.FP.PNG_V03.
[22] Y. Li, M. Li, C. Dang, X. Liu, Effects of dissolved gas on the nucleation and growth of ice crystals in freezing droplets, Int. J. Heat Mass Tran. 184 (2022), 122334, https://doi.org/10.1016/J.IJHEATMASSTRANSFER.2021.122334.
[23] C. Lyu, G. Nastase, G. Ukpai, A. Serban, B. Rubinsky, A comparison of freezing-damage during isochoric and isobaric freezing of the potato, PeerJ 5 (2017), e3322, https://doi.org/10.7717/peerj.3322.
[24] P.M. Mehl, Nucleation and crystal growth in a vitrification solution tested for organ cryopreservation by vitrification, Cryobiology 30 (1993) 509–518, https://doi.org/10.1006/cryo.1993.1051.
[25] D.A. Noday, P.S. Steif, Y. Rabin, Viscosity of cryoprotective agents near glass transition: a new device, technique, and data on DMSO, DP6, and VS55, Exp. Mech. 49 (2009) 663–672, https://doi.org/10.1007/s11340-008-9191-8.
[26] P.A. Perez, J. Preciado, G. Carlson, R. DeLonzor, B. Rubinsky, The effect of undissolved air on isochoric freezing, Cryobiology 72 (2016) 225–231, https://doi.org/10.1016/J.CRYOBIOL.2016.04.002.
[27] J. Plitz, Y. Rabin, J.R. Walsh, The effect of thermal expansion of ingredients on the cocktails VS55 and DP6, Cell Preserv. Technol. 2 (2004) 215–226, https://doi.org/10.1089/cpt.2004.2.215.
[28] M.J. Powell-Palm, V. Charwat, B. Charrez, B. Siemons, K.E. Healy, B. Rubinsky, Isochoric supercooled preservation and revival of human cardiac microtissues, Commun. Biol. 41 (4) (2021) 1–7, https://doi.org/10.1038/s42003-021-02650-9, 2021.
[29] M.J. Powell-Palm, Y. Zhang, J. Aruda, B. Rubinsky, Isochoric conditions enable high subfreezing temperature pancreatic islet preservation without osmotic cryoprotective agents, Cryobiology 86 (2019) 130–133, https://doi.org/10.1016/J.CRYOBIOL.2019.01.003.
[30] J. Preciado, B. Rubinsky, The effect of isochoric freezing on mammalian cells in an extracellular phosphate buffered solution, Cryobiology 82 (2018) 155–158, https://doi.org/10.1016/J.CRYOBIOL.2018.04.004.
[31] J.A. Preciado, B. Rubinsky, Isochoric preservation: a novel characterization method, Cryobiology 60 (2010) 23–29, https://doi.org/10.1016/J.CRYOBIOL.2009.06.010.
[32] Y. Rabin, J. Plitz, Thermal expansion of blood vessels and muscle specimens permeated with DMSO, DP6, and VS55 at cryogenic temperatures, Ann. Biomed. Eng. 33 (2005) 1213–1228, https://doi.org/10.1007/s10439-005-5364-0.
[33] Y. Rabin, P.S. Steif, K.C. Hess, J.L. Jimenez-Rios, M.C. Palastro, Fracture formation in vitrified thin films of cryoprotectants, Cryobiology 53 (2006) 75–95, https://doi.org/10.1016/j.cryobiol.2006.03.013.
[34] Y. Rabin, M.J. Taylor, J.R. Walsh, S. Baicu, P.S. Steif, Cryomacroscopy of vitrification I: a prototype and experimental observations on the cocktails VS55 and DP6, Cell Preserv. Technol. 3 (2005) 169–183, https://doi.org/10.1089/cpt.2005.3.169.
[35] J.L.J. Rios, Y. Rabin, Thermal expansion of blood vessels in low cryogenic temperatures Part I: a new experimental device, Cryobiology 52 (2006) 269–283, https://doi.org/10.1016/J.CRYOBIOL.2005.12.005.
[36] B. Rubinsky, P.A. Perez, M.E. Carlson, The thermodynamic principles of isochoric cryopreservation, Cryobiology 50 (2005) 121–138, https://doi.org/10.1016/J.CRYOBIOL.2004.12.002.
[37] D. Saury, S. Harmand, M. Siroux, Experimental study of flash evaporation of a water film, Int. J. Heat Mass Tran. 45 (2002) 3447–3457, https://doi.org/10.1016/S0017-9310(02)00056-X.
[38] N.O. Smith, The difference between Cp and Cv for liquids and solids, J. Chem. Educ. 42 (1965) 654–655, https://doi.org/10.1021/ED042P654.
[39] P.K. Solanki, Y. Rabin, PERSPECTIVE: temperature-dependent density and thermal expansion of cryoprotective cocktails, Cryo Lett. 43 (2022) 1–9.
[40] P.K. Solanki, J.C. Bischof, Y. Rabin, Thermo-mechanical stress analysis of cryopreservation in cryobags and the potential benefit of nanowarming, Cryobiology 76 (2017) 129–139, https://doi.org/10.1016/j.cryobiol.2017.02.001.
[41] P.K. Solanki, Y. Rabin, Thermo-mechanics aspects of isochoric cryopreservation: a new modeling approach and comparison with experimental data, PLoS One 17 (2022), e0267852, https://doi.org/10.1371/JOURNAL.PONE.0267852.
[42] P. Solanki, Y. Rabin, Scaling effects on the residual thermomechanical stress during ice-free cooling to storage temperature, J. Appl. Mech. 87 (2020), 101003, https://doi.org/10.1115/1.4047420.
[43] P.S. Steif, D.A. Noday, Y. Rabin, Can thermal expansion differences between cryopreserved tissue and cryoprotective agents alone cause cracking? Cryo-Letters 30 (2009) 414–421.
[44] P.S. Steif, M.C. Palastro, Y. Rabin, The effect of temperature gradients on stress development during cryopreservation via vitrification, Cell Preserv. Technol. 5 (2007) 104–115, https://doi.org/10.1089/cpt.2007.9994.
[45] G.J. Suppes, S. Egan, A.J. Casillan, K.W. Chan, B. Seckar, Impact of high pressure freezing on DH5α Escherichia coli and red blood cells, Cryobiology 47 (2003) 93–101, https://doi.org/10.1016/S0011-2240(03)00072-5.
[46] T. Takahashi, A. Kakita, Y. Takahashi, I. Sakamoto, K. Yokoyama, T. Fujiu, S. Yamashina, T. Tamaki, Y. Takazawa, R. Muratsubaki, Functional integrity of the rat liver after subzero preservation under high pressure, Transplant. Proc. 32 (2000) 1634–1636, https://doi.org/10.1016/S0041-1345(00)01440-8.
[47] M.J. Taylor, B.P. Weegman, S.C. Baicu, S.E. Giwa, New approaches to cryopreservation of cells, tissues, and organs, Transfus. Med. Hemotherapy 46 (2019) 197–215, https://doi.org/10.1159/000499453.
[48] L. Wan, M.J. Powell-Palm, C. Lee, A. Gupta, B.P. Weegman, M.G. Clemens, B. Rubinsky, Preservation of rat hearts in subfreezing temperature isochoric conditions to – 8 °C and 78 MPa, Biochem. Biophys. Res. Commun. 496 (2018) 852–857, https://doi.org/10.1016/J.BBRC.2018.01.140.
[49] Y. Zhang, G. Ukpai, A. Grigoropoulos, M.J. Powell-Palm, B.P. Weegman, M. J. Taylor, B. Rubinsky, Isochoric vitrification: an experimental study to establish proof of concept, Cryobiology 83 (2018) 48–55, https://doi.org/10.1016/J.CRYOBIOL.2018.06.005.